

# On Instability in Gas Lift Wells and Schemes for Stabilization by Automatic Control

Gisle Otto Eikrem, SPE, Ole Morten Aamo, and Bjarne A. Foss, Norwegian University of Science and Technology

## Summary

In this paper, we present a simple nonlinear dynamic model that is shown to capture the essential dynamics of the casing-heading instability in gas lift wells despite the complex nature of two-phase flow. Using the model, stability maps are generated showing regions of stable and unstable settings for the production valve governing the flow of produced oil and gas from the tubing. Optimal steady-state production is shown to lie well within the unstable region, corresponding to an oil-production rate that cannot be sustained without automatic control. Three simple control structures are suggested that successfully stabilize the casing-heading instability in simulations, and more importantly in laboratory experiments.

## Introduction

Artificial lift is a common technique to increase tail-end production from mature fields, and injection of gas is among the most widely used methods. Gas is injected into the tubing as deep as possible and mixes with the fluid from the reservoir (see Fig. 1). Because the gas has lower density than the reservoir fluid, the density of the fluid in the tubing and, consequently, the downhole pressure decrease. As the downhole pressure decreases, the production from the reservoir increases. The lift gas is routed from the surface and into the annulus, which is the volume between the casing and the tubing, and enters the tubing through a valve, or an injection orifice. Backflow from the tubing into the annulus is not permitted by this valve. Gas lift can induce severe production flow oscillations because of casing-heading instability, a phenomenon that originates from dynamic interaction between injection gas in the casing and the multiphase fluid in the tubing. The fluctuating flow typically has an oscillation period of a few hours and is distinctly different from short-term oscillations caused by hydrodynamic slugging. The casing-heading instability introduces two production-related challenges. Average production is decreased as compared to a stable-flow regime and the highly oscillatory flow puts strain on downstream equipment. Reports from industry as well as academia suggest that automatic control (feedback control) is a powerful tool to eliminate casing-heading instability and increase production from gas lift wells (Kinderen and Dunham 1998; Jansen et al. 1999; Dalsmo et al. 2002; Boisard et al. 2002; Hu and Golan 2003; Eikrem et al. 2006; Aamo et al. 2005).

Understanding and predicting conditions under which a gas lift well will exhibit flow instability is important in every production-planning situation. This problem has been addressed by several authors by constructing stability maps, [i.e., a 2D diagram that shows the regions of stable and unstable production of a well (Eikrem et al. 2006; Poblano et al. 2005; Fairuzov et al. 2004)]. The axes may define the operating conditions in terms of gas-injection rate and production-choke opening or wellhead pressure.

In this paper, we present three different control structures for stabilizing casing-heading instability in gas lift wells. Stability is analyzed for each controller, and it is shown how feedback control stabilizes performance, at least locally, around some operating

point. The performance of the controllers is demonstrated in simulations, but more importantly, stabilization is also achieved in laboratory experiments.

The paper is organized as follows: A description of the laboratory facilities that are used in this work is given. Thereafter, the dynamics of casing-heading instability are discussed, and suitable models for analysis and design are proposed. The proposed control structures are presented along with stability analysis, closed-loop simulations, and experimental results. The paper ends with conclusions.

## The Gas Lift Laboratory at Delft University of Technology (DUT)

Realistic tests of control structures for gas lift wells are performed using the gas lift well laboratory setup at TU Delft.\* The laboratory installation represents a dual gas lift well, using compressed air as lift gas and water as produced fluid. It is shown in Fig. 2. Only the long tubing is used in the experiments (single gas lift well), hence only this part is described. The production tube is transparent, facilitating visual inspection of the flow phenomena occurring as control is applied. It measures 18 m in height and has an inner diameter of 20 mm, see Fig. 2a. The fluid reservoir is represented by a tube of the same height, but with a substantially larger inner diameter of 80 mm. The reservoir pressure is given by the static height of the fluid in the reservoir tube. A gas bottle represents the annulus, as shown in Fig. 2b. In the experiments run in this study, gas is fed into the annulus at a constant rate of  $0.6 \times 10^{-3}$  kg/s. Input and output signals to and from the installation are handled by a microcomputer system, see Fig. 2c, to which a laptop computer is interfaced for running the control algorithm and presenting output. The sampling time is 1 second.

## Casing-Heading Instability

This section discusses casing-heading instability and presents a nonlinear dynamic model suitable for analysis.

**Explaining the Phenomenon.** The dynamics of highly oscillatory flow in single-point-injection gas lift oil wells can be described as follows:

- Gas from the annulus starts to flow into the tubing. As gas enters the tubing, the pressure in the tubing falls, accelerating the inflow of lift gas.
- If there is uncontrolled gas passage between the annulus and tubing, the gas pushes the major part of the liquid out of the tubing, while the pressure in the annulus falls dramatically.
- The annulus is practically empty, leading to a negative pressure difference over the injection orifice, blocking the gas flow into the tubing. Because of the blockage, the tubing becomes filled with liquid and the annulus with gas.
- Eventually, the pressure in the annulus becomes high enough for gas to penetrate into the tubing, and a new cycle begins.

For more information on this type of instability, also termed severe slugging, see (Xu and Golan 1989). The oscillating production causes problems for downstream processing equipment, and

\* The experimental setup is designed and implemented by Shell International Exploration and Production B.V., Rijswijk, and is now located in the Kramers Laboratorium voor Fysische Technologie, Faculty of Applied Sciences, Delft University of Technology.

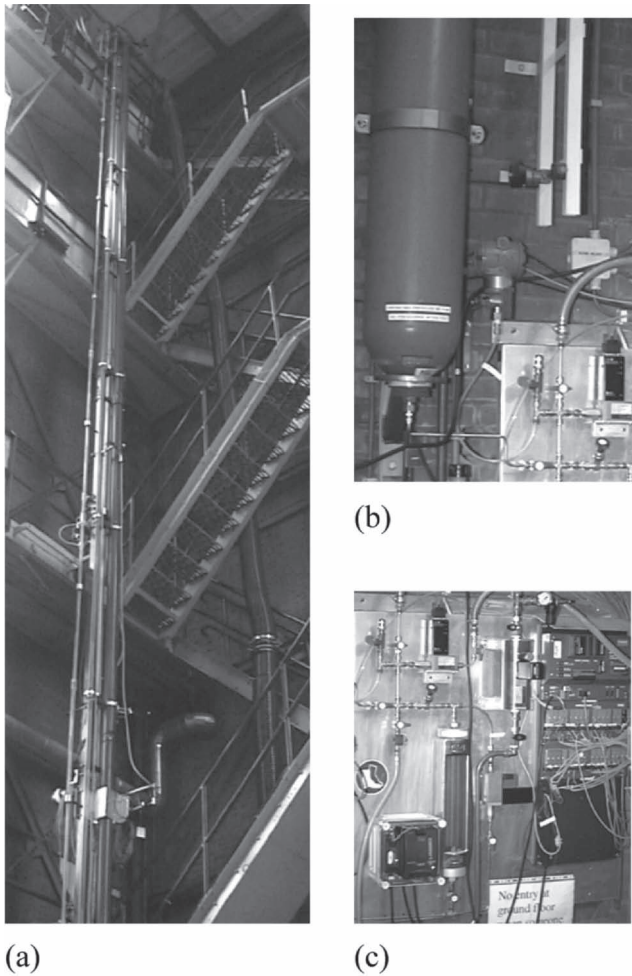


Fig. 1—A gas lift oil well.

may be unacceptable in operations. The traditional remedy is to choke back to obtain a non-oscillating flow. As mentioned in the introduction, automatic control is a powerful approach to eliminate oscillations. Moreover, reports also show that this technology increases production (Kinderen and Dunham 1998; Jansen et al. 1999; Dalsmo et al. 2002; Boisard et al. 2002; Hu and Golan 2003; Eikrem et al. 2006; Aamo et al. 2005). Another approach is to fit a gas lift valve that secures critical flow. This decouples the dynamics of the casing and tubing volumes and thereby eliminates casing-heading instabilities.

**A Nonlinear Dynamic Model.** The process is modeled by three states:  $x_1$  is the mass of gas in the annulus;  $x_2$  is the mass of gas in the tubing, and  $x_3$  is the mass of oil above the gas injection point in the tubing. Looking at Fig. 1,

$$\dot{x}_1 = w_{gc} - w_{iv}, \dots \dots \dots (1)$$

$$\dot{x}_2 = w_{iv} + w_{rg} - w_{pg}, \dots \dots \dots (2)$$

$$\dot{x}_3 = w_{ro} - w_{po}, \dots \dots \dots (3)$$

where  $\dot{\cdot}$  denotes differentiation with respect to time, and  $w_{gc}$  is a constant mass flow rate of lift gas into the annulus,  $w_{iv}$  is the mass flow rate of lift gas from the annulus into the tubing,  $w_{rg}$  is the gas mass flow rate from the reservoir into the tubing,  $w_{pg}$  is the mass flow rate of gas through the production choke,  $w_{ro}$  is the oil mass flow rate from the reservoir into the tubing, and  $w_{po}$  is the mass flow rate of produced oil through the production choke. The detailed expressions for the flows occurring in Eqs. 1 through 3 are given in the Appendix.

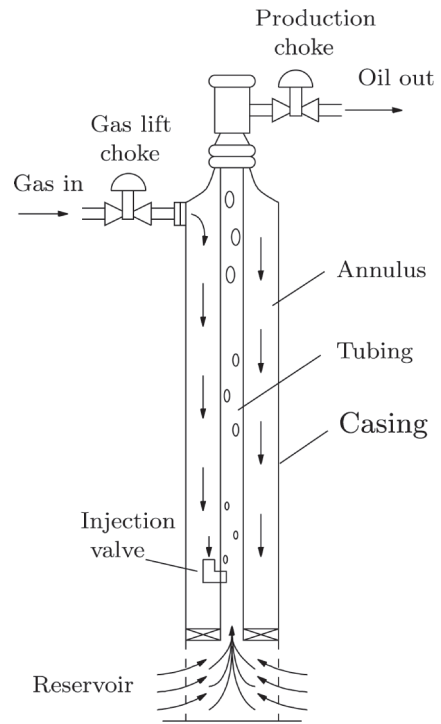


Fig. 2—Sketch of the gas lift laboratory, (a) The production tubes, (b) the annulus volume, and (c) the microcomputer.

**A Linearized Dynamic Model.** A linear version of the nonlinear model previously presented will be derived here.

Given a production choke opening  $u = u^*$ , we look for a steady-state solution  $x = [x_1 \ x_2 \ x_3] = x^*$  that solves Eqs. 1 through 3 when the time derivatives on the left hand side are set equal to zero. This solution has a corresponding steady oil production flow. This flow, however, may be unstable so that it cannot be sustained in practice when various disturbances are present. Eqs. 1 through 3 are linearized around  $(x^*, u^*)$  to obtain the system

$$\Delta \dot{x} = A \Delta x + B \Delta u, \dots \dots \dots (4)$$

where  $\Delta x = x - x^*$ ,  $\Delta u = u - u^*$ , and  $A$  and  $B$  are  $3 \times 3$  and  $3 \times 1$  matrices, respectively.

**Automatic Control**

In this section, control structures will be proposed and studied using tools for stability analysis. In addition, the performance of the proposed controllers will be demonstrated in simulations using the nonlinear model previously presented as well as using OLGA<sup>®</sup> 2000 that represents the state-of-the-art in multiphase flow simulation.\*

Finally, constituting the main findings of this paper, results from laboratory experiments will be presented that prove the feasibility of applying the proposed control strategies in practice. In all cases presented, a PI-controller will be employed. Its transfer function is given by

$$H_C(s) = K_p \left( 1 + \frac{1}{\tau_I s} \right), \dots \dots \dots (5)$$

where  $K_p$  is the proportional gain,  $\tau_I$  is the integral time and  $s$  is the Laplace variable. The controller includes integrator windup to limit the effect of the integral term when the control input,  $u$ , saturates.

\* OLGA is a registered trademark of the SPT Group, Kjeller, Norway.

$$\Delta y = C_{\text{tub}} \Delta x, \dots \dots \dots (6)$$

can be derived where  $\Delta x = x - x^*$ ,  $\Delta y = y_{\text{tub}} - y_{\text{tub}}^*$ , and  $C_{\text{tub}}$  is a  $1 \times 3$  matrix.

The system analysis takes place in the frequency domain, making use of the transfer function from control input  $\Delta u$  to output  $\Delta y$ . The transfer function is obtained from Eqs. 4 and 6 by noting that  $\Delta \dot{x} = s \Delta x$ .

$$H_{y,u^*}(s) = C_{\text{tub}}(sI - A)^{-1}B. \dots \dots \dots (7)$$

The subscript  $u^*$  reflects the fact that the transfer function can be parameterized by the steady-state production-choke opening.

Here, the setpoint is chosen as  $y_{\text{tub}}^* = 1.7$  bara, which corresponds to  $u^* = 82.5\%$ . With the transfer function established with Eq. 7, the next step is to design the parameters of the PI controller. The stabilizing component of the controller is its proportional gain  $K_p$ . For sufficiently large  $\tau_I$  the integral part has effect at only very low frequencies, and is therefore disregarded when designing  $K_p$ . For the design of  $K_p$ , the Nyquist stability criterion is employed. This well-known tool is an application of the argument principle of complex analysis and lends itself particularly useful for choosing  $K_p$ . It states that the graph of the complex loop transfer function

$H_{y,u^*}(j\omega)$  should encircle the point  $-\frac{1}{K_p}$  on the real axis  $N = Z - P$  times in the clockwise direction as  $\omega$  runs from  $-\infty$  to  $\infty$  ( $j$  is the imaginary unit).  $Z$  and  $P$  are, respectively, the number of zeros and the poles of  $H_{y,u^*}(s)$  that lie in the right half of the complex plane (Franklin et al. 2002). The Nyquist plot for this case is shown in Fig. 4, where the solid line represents the time-continuous case, while the dashed line represents the time-discrete case with a sampling interval of 1 second. The  $\times$  identifies the point  $-\frac{1}{K_p}$  for  $K_p = 1$ .

As can be seen from the figure, the interval  $(-1.2, 0)$  on the real axis is encircled twice by the solid line, and the interval  $(-1.2, -0.2)$  is encircled twice by the dashed line. It follows that for stability,  $K_p$  must lie in the interval  $(0.8, 5)$ . Notice that the lower bound on  $K_p$  comes from the properties of the system because feedback control is necessary to maintain stable production. The upper bound on  $K_p$  is a result of discretization and can be increased by making the sampling interval shorter. The controller gain for this case is selected as  $K_p = 3$ . With the controller gain selected,

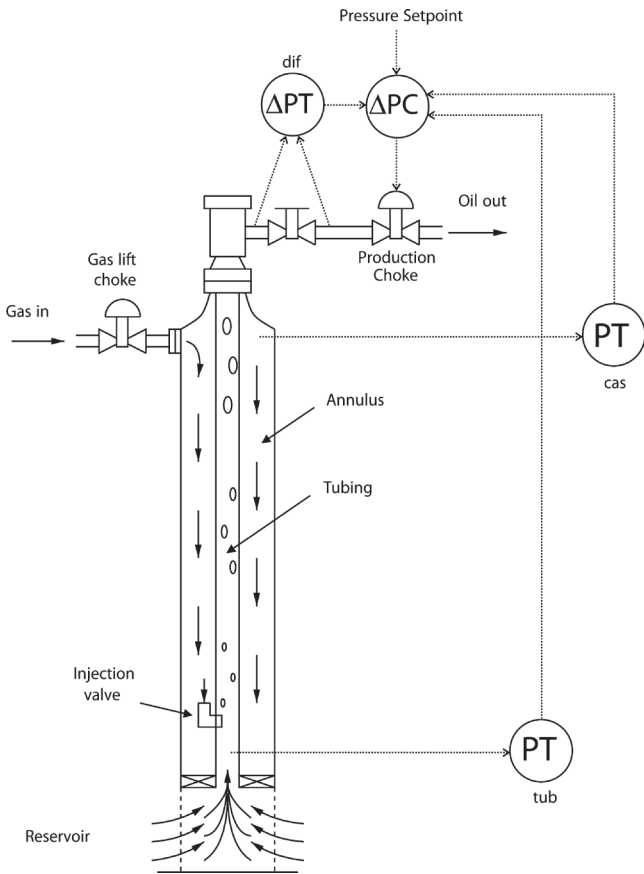


Fig. 3—The three control structures (PT=Pressure Transmitter, PC=Pressure Controller).

**Stabilization Using Downhole Pressure. Controller Design and Linear Analysis.** In this section, a possible control structure for stabilization of gas lift wells based on measuring the downhole pressure  $y_{\text{tub}}$ , is investigated. As in all cases studied, the means of actuation is the production choke, giving the control structure marked “tub” in Fig. 3. Given a desired setpoint  $y_{\text{tub}}^*$ , the corresponding steady state is denoted  $(x^*, u^*)$ . A linearized output

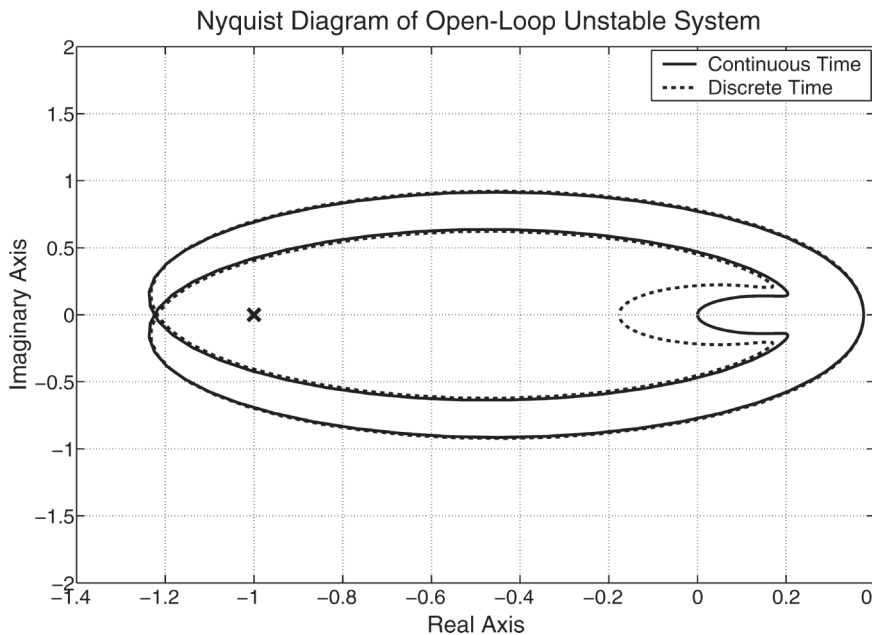


Fig. 4—The Nyquist diagram of the open-loop transfer function for  $u^* = 82.5\%$ .

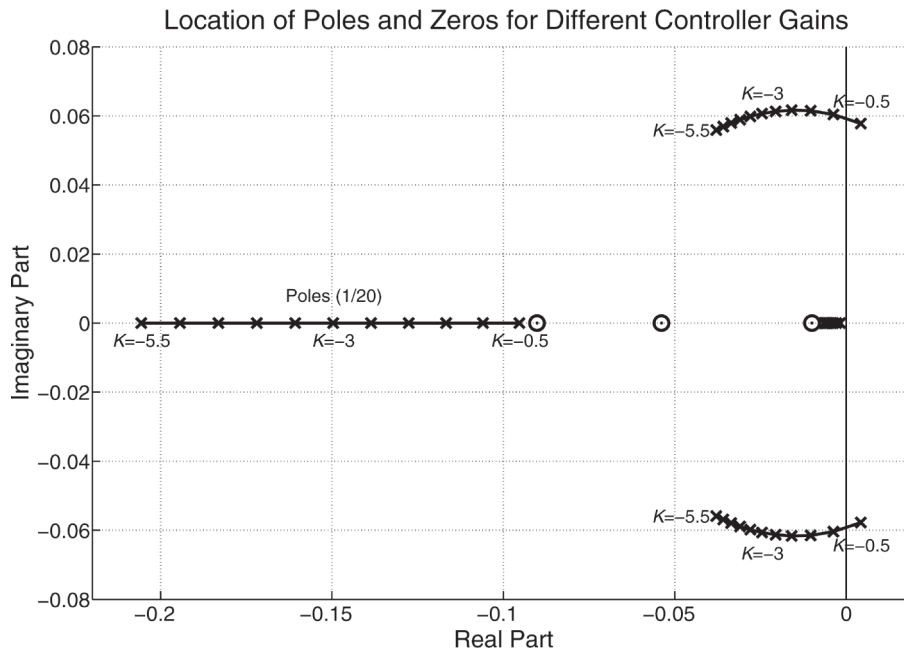


Fig. 5—The location of the closed-loop poles for different controller gains  $K_p, u^*=82.5\%$ .

the integral time is selected to obtain a desired rate at which to compensate for steady-state error. Simulations suggest that  $\tau_I = 100$  sec is a reasonable choice. Fig. 5 shows the location of closed-loop poles as a function of  $K_p$ . For large values of  $K_p$ , all poles are located in the left half of the complex plane. As  $K_p$  fails to provide local stability for all  $u^*$  because of nonlinear effects, indicating that a (nonlinear) gain-scheduling controller may be necessary. This is consistent with the Nyquist plot. Fig. 6 investigates the capability of the controller designed for  $u^* = 82.5\%$  to stabilize other steady states locally. It shows the location of closed-loop poles as functions of steady state given in terms of production-choke opening  $u^*$ . As the steady-state production choke opening is increased, two poles (complex conjugated) move toward the right and cross into the right half of the complex plane at  $u^* \approx 96\%$ . One interpretation of this result is that the system is not controllable

for large valve opening because the pressure drop over the production choke becomes too small. Hence, there is not sufficient control authority to stabilize the casing-heading instability. A second interpretation is that the controller designed for  $u^* = 82.5\%$  fails to provide local stability for all  $u^*$  because of nonlinear effects, indicating that a (nonlinear) gain-scheduling controller may be necessary.

**Simulation Results.** The analysis of the closed-loop system indicates that the designed controller will stabilize the unstable gas lift well. On the basis of these results, simulations of the closed-loop system are performed in this section.

**Simplified Model.** Simulations using the simplified model previously presented have been performed using the model parameters given in Table 1 and the controller parameters given in Table 2. Gain scheduling is used to improve performance. In this

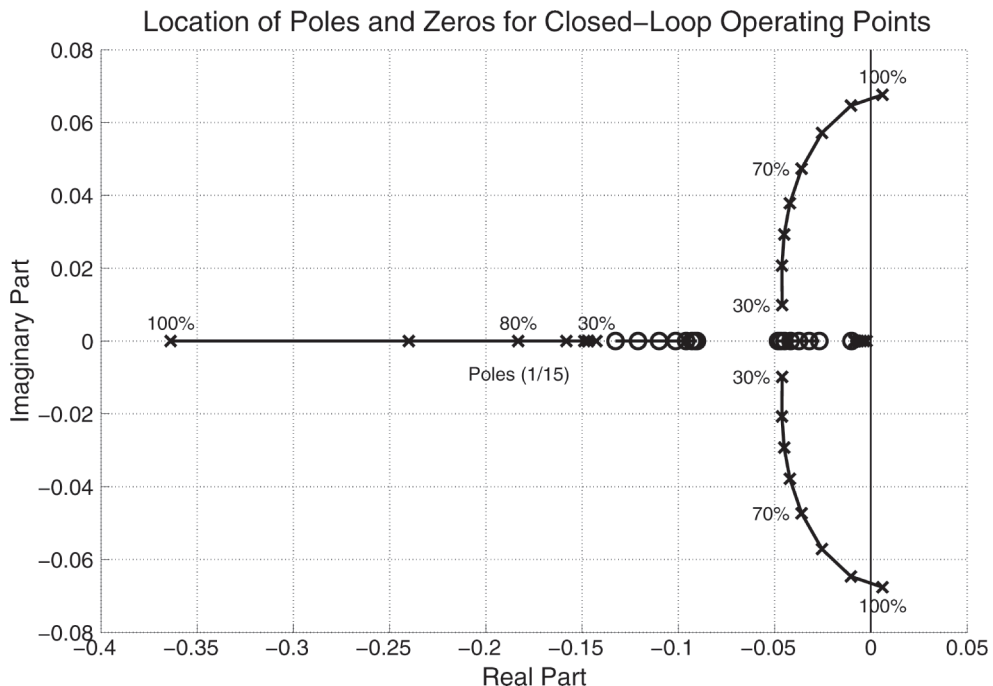


Fig. 6—The location of the closed-loop poles for different operating points  $u^*$ . Controller parameters are  $K_p=3$  and  $\tau_I=100$  seconds.

**TABLE 1—NUMERICAL COEFFICIENTS**

| Parameter | Value                  | Unit              |
|-----------|------------------------|-------------------|
| $M$       | 0.028                  | kg/mol            |
| $R$       | 8.31                   | J/Kmol            |
| $g$       | 9.81                   | m/s <sup>2</sup>  |
| $T_a$     | 293                    | K                 |
| $L_a$     | 0.907                  | m                 |
| $V_a$     | $22.3 \times 10^{-3}$  | m <sup>3</sup>    |
| $\rho_o$  | 1000                   | kg/m <sup>3</sup> |
| $p_s$     | $1 \times 10^5$        | Pa                |
| $w_{gc}$  | $0.6 \times 10^{-3}$   | kg/s              |
| $p_r$     | $2.9 \times 10^5$      | Pa                |
| $T_w$     | 293                    | K                 |
| $L_w$     | 14                     | m                 |
| $L_r$     | 4                      | m                 |
| $A_w$     | $0.314 \times 10^{-3}$ | m <sup>2</sup>    |
| $A_r$     | $0.314 \times 10^{-3}$ | m <sup>2</sup>    |
| $C_{iv}$  | $1.60 \times 10^{-6}$  | m <sup>2</sup>    |
| $C_{pc}$  | $0.156 \times 10^{-3}$ | m <sup>2</sup>    |
| $C_r$     | $12 \times 10^{-6}$    | m <sup>2</sup>    |
| $r_{go}$  | 0                      | —                 |

case, gain scheduling means that the gain  $K_p$  changes according to the production choke opening.

The simulation sequence is as follows (see also Table 3): After keeping the choke at 50% for 10 min, the downhole pressure is at 1.97 bara and total production is at 5.3 kg/min (both almost steady), see Figs. 7 and 8. When the controller is turned on after 10 min, the downhole pressure is reduced from 1.97 to 1.70 bara as the controller gently opens the production choke from 50 to 82.5%. The total production from the gas lift well increases from 5.3 to 5.9 kg/min because of the reduced downhole pressure. The casinghead pressure is reduced from 2.01 bara to 1.74 bara, while the tubinghead pressure is reduced from 1.27 to 1.04 bara in the same time period, see Fig. 9. Because the gas supply into the annulus is kept at a constant rate, the increase in total production between the two steady states  $u^*=50\%$  and  $u^*=82.5\%$  actually represents an increase in oil production. Notice in the figures that the system goes into severe slugging when the controller is turned off, and a small disturbance is introduced after 35 min. The controller is turned off only to demonstrate that steady flow cannot be sustained without automatic control—in practice, control must be active at all times. This is consistent with the results from the linear analysis as shown in Fig. 4.

Additional simulations were carried out to test robustness of the control system. It was observed that the controller was able to stabilize the system even from severe slugging operation, indicating that choking back to obtain steady flow before turning the controller on is not necessary in this case. However, it turns out to be necessary in practice, as shown later.

**OLGA 2000 Model.** Although the simulation study above using the simplified gas lift model gave promising results for the chosen control structure, here a more realistic test is carried out by applying the control structure to an OLGA 2000 model of the laboratory-scale gas lift well. The simulation of the closed-loop system uses the control sequence given in Table 3, and the controller parameters given in Table 4. To achieve satisfactory performance, the controller parameters had to be tuned as a higher gain was needed in the OLGA 2000 simulations.

**TABLE 2—CONTROLLER PARAMETERS FOR PI-CONTROLLER USED IN SIMULATIONS WITH THE SIMPLIFIED MODEL**

| Choke Opening            | Gain $K_p$ | Integral Time $\tau_i$ |
|--------------------------|------------|------------------------|
| $50\% \leq u \leq 75\%$  | $\leq 2$   | 200 sec                |
| $75\% \leq u \leq 100\%$ | 3          | 200 sec                |

The simulation results are given in Figs. 10 through 12. Choking back to 55% over a period of 10 min brings the system into a steady state with a total production of approximately 2 kg/min. As the controller gently increases the choke opening from 50 to 88%, the downhole pressure is reduced from 2.70 to 2.20 bara, causing the total production to increase from 2 kg/min to approximately 4 kg/min. The tubinghead pressure is reduced from 1.75 to 1.23 bara, and the casinghead pressure is reduced from 1.7 to 1.25 bara in the same time period. Notice that the system quickly goes into severe slugging when the controller is turned off after 35 min, confirming that the chosen steady state is indeed open-loop unstable.

**Experimental Results.** Motivated by the promising results obtained in simulations, experimental tests were performed in the gas lift laboratory. The experiment uses the control sequence shown in Table 5, and the control parameters shown in Table 6. The control parameters were retuned to improve performance.

A representative set of results from the laboratory experiments is given in Figs. 13 through 15. As the controller opens the production choke from 55 to 82.5%, the downhole pressure is reduced from 2.53 to 2.18 bara. As a result, the total production is increased from approximately 2 kg/min to approximately 4.5 kg/min. The tubinghead pressure is reduced from 1.51 to 1.19 bara, and the casinghead pressure is reduced from 2.65 to 2.30 bara in the same time period. The controller achieves regulation to the desired setpoint, and the setpoint represents an open-loop unstable steady state as shown by the oscillations appearing when the controller is turned off after 25 min. While stabilization was achieved from initial conditions far from the steady state in simulations, this is not the case in the experiments. Here, the control sequence of Table 5 proved necessary for achieving stabilization, as opposed to the simulation results using the simplified model. This deterioration of robustness is common when moving from idealistic models with numerous simplifications to real plants, and it does not present a restriction to the applicability of the controller because, one in practice, one always will follow a control sequence similar to the two first lines of Table 5. In conclusion, the experiment shows that the controller performs well and that it has the potential of increasing production significantly.

**Stabilization Using Casinghead Pressure.** In this section, a control structure based on measuring the casing head pressure  $y_{cas}$ , is investigated. Again, the means of actuation is the production choke, giving the control structure marked “cas” in Fig. 3. For a given setpoint  $y_{cas}^*$ , a linearized output, as in Eq. 6, and a corresponding transfer function as in Eq. 7, can be derived.

The results using the casinghead pressure follow the results using the downhole pressure. Linear analysis shows that there is

**TABLE 3—CONTROL SEQUENCE FOR SIMULATION TRIALS**

| Time Slot     | Control Mode | Choke Opening  |
|---------------|--------------|----------------|
| 0 min–10 min  | Open loop    | 50.0% (simple) |
|               |              | 55.0% (OLGA)   |
| 10 min–35 min | Closed loop  | Controlled     |
| 35 min–45 min | Open loop    | 82.5% (simple) |
|               |              | 88.0% (OLGA)   |

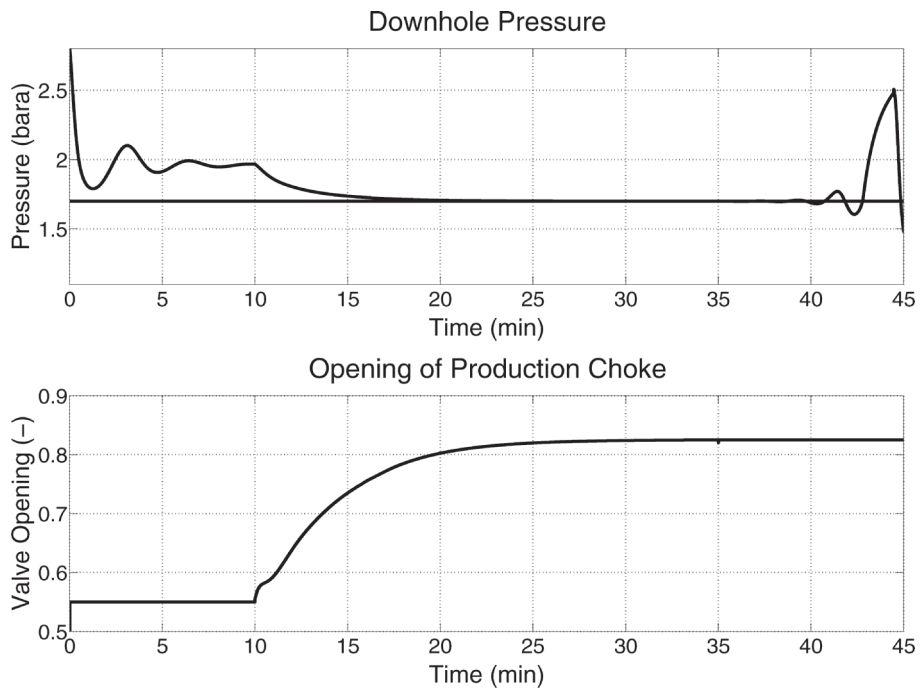


Fig. 7—(a) Downhole pressure and (b) production-choke opening for simulation with the simplified model.

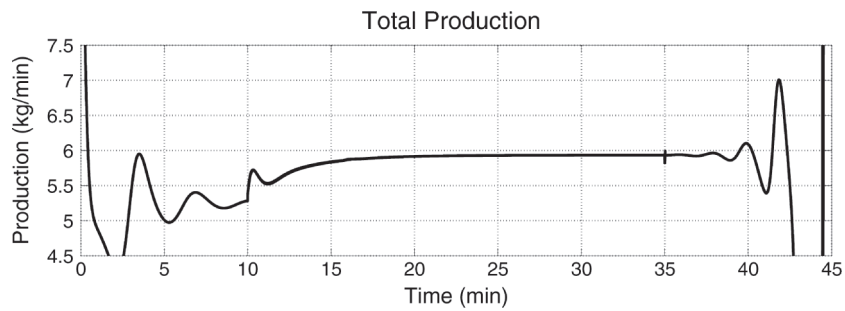


Fig. 8—Total production for simulation with the simplified model.

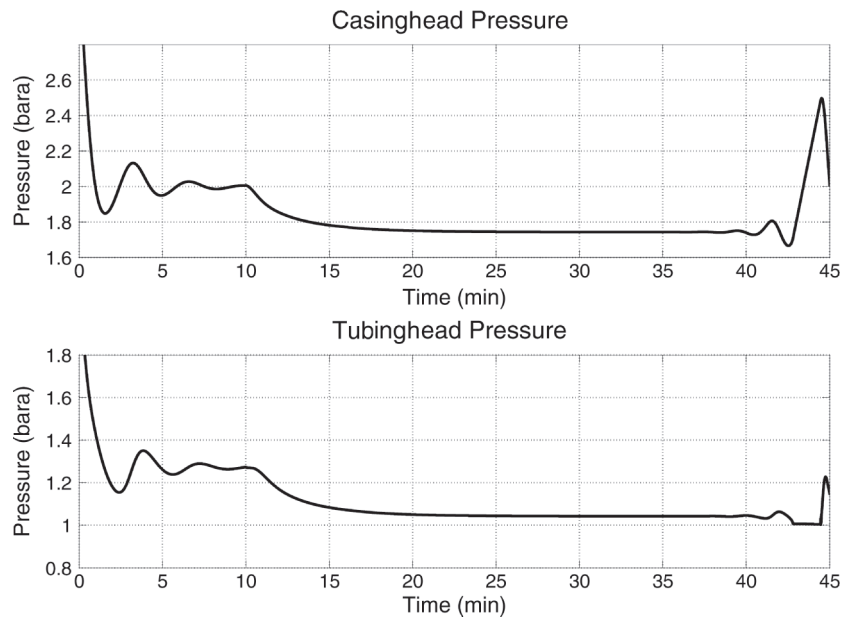


Fig. 9—(a) Casinghead pressure and (b) tubinghead pressure for simulation with the simplified model.

**TABLE 4—CONTROLLER PARAMETERS FOR PI-CONTROLLER USED IN SIMULATIONS WITH OLGA 2000**

|                          | Gain  | Integral Time |
|--------------------------|-------|---------------|
| Choke Opening            | $K_p$ | $\tau_I$      |
| $50\% \leq u \leq 75\%$  | 5     | 100 sec       |
| $75\% \leq u \leq 100\%$ | 9     | 100 sec       |

a lower and upper bound on the gain  $K_p$ , and nonlinearities imply that it is advantageous to apply gain-scheduling control. Further, the gains chosen for the simplified model need to be adjusted when applied to the OLGA 2000 simulator and in experiments. To provide a flavor for the results, a representative result is shown in Fig. 16. This experiment, again, follows the sequence outlined in Table 5. The casinghead pressure settles at its setpoint value of 2.30 bara roughly 15 minutes after the control loop has been closed. Furthermore, it is clear from Fig. 16 that casing-heading oscillations appear shortly after the controller is deactivated.

**Stabilization Using Differential Pressure.** The outset for the third control structure is the use of a differential-pressure measurement to stabilize casing-heading instability. This may be viewed as a way of controlling the production flow rate. The control structure is marked “dif” in Fig. 3. Some comments need to be made related to experimental results. First, the differential-pressure measurement  $y_{dif}$  is measured across a restriction in front of the production choke. A typical result is shown in Fig. 17. Again, the controller stabilizes the flow. It should, however, be noted that the variation in the production-choke opening is much larger than for the other controllers, see Fig. 13 and Fig. 16.

The reason for this difference is a higher noise level on the differential pressure measurement than on the downhole-pressure measurement and the casing-head pressure measurement. The noise level can be reduced using a lowpass filter with a lower cutoff frequency than the currently implemented lowpass filter. The filter can be implemented without reducing controller performance because the bandwidth of the controller is on the order of several minutes and the sampling time is 1 second.

## Conclusions

This investigation has shown that automatic control is a feasible option for optimizing production from gas lift wells suffering from casing-head instability. In particular, it has been shown that different control structures can be applied to the same well with similar performance. This is a positive result because it is possible to switch from one control structure to another in the event of sensor failure, for instance, by switching from downhole pressure to casinghead pressure.

Hence, the design of a backup strategy is straightforward. Moreover, the algorithms used in the different cases are equal: simple PI-controller algorithms. This means that a change from one control structure to another implies only the change of a few controller parameters.

The results indicate that gain-scheduling control improves performance. This is commonly used in industry. It may, however, be possible to alleviate the need for gain scheduling by including a cascaded loop where the stabilizing controller sees the setpoint of an inner flow loop as its control input rather than the production-choke opening.

Among the control structures studied, the casinghead pressure and the downhole pressure are the best choices for stabilization of slug flow, as their robustness properties seem to be superior. If neither of these measurements is available, the pressure drop across a restriction upstream of the production choke can be applied. Increased robustness can be obtained through redundancy the case two or more of the measurements are available, as previously discussed. It should be noted, this work is limited to the use of the production choke as the control input. An alternative control input would be the gas lift choke, which is a topic for further research.

We hope this study contributes to the understanding of casing-heading instability through its emphasis on a mix of analysis and trials. The consistency of the findings, between linear analysis and experimental results, indicates that a mixed approach should be useful also for other similar applications.

## Acknowledgments

We acknowledge the support from Shell International Exploration and Production B.V. and Kramers Laboratorium voor Fysische Technologie, Faculty of Applied Sciences, DUT. In particular, we would like to thank Richard Fernandes (Shell) and R.V.A. Olie-mans (DUT). Further, we acknowledge the support from ABB

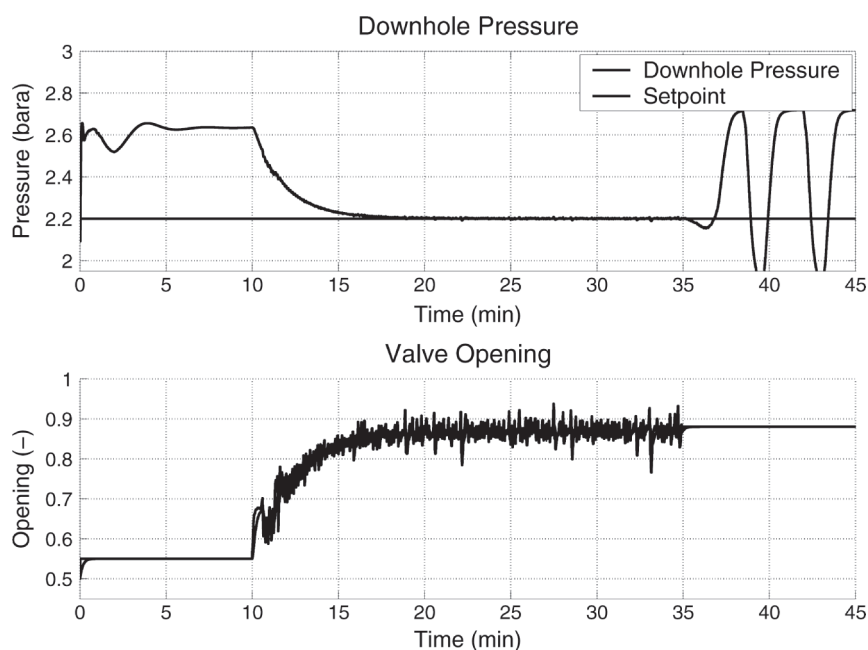


**Fig. 10—(a) Downhole pressure and (b) production-choke opening for simulation with OLGA 2000.**

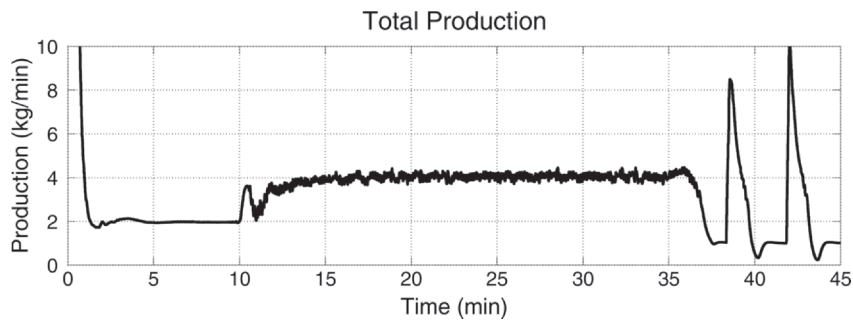


Fig. 11—Total production for simulation with OLGA 2000.

A/S, Hydro ASA, and the Research Council of Norway through the Petronics program.

**Nomenclature**

- $A_r$  = cross-sectional area of tubing below the gas injection point, [L<sup>2</sup>], m<sup>2</sup>
- $A_w$  = cross-sectional area of tubing above the gas injection point, [L<sup>2</sup>], m<sup>2</sup>
- $C_{iv}$  = valve constant for gas-injection valve, [L<sup>2</sup>], m<sup>2</sup>
- $C_{pc}$  = valve constant for production valve, [L<sup>2</sup>], m<sup>2</sup>
- $C_l$  = valve constant for reservoir valve, [L<sup>2</sup>], m<sup>2</sup>
- $\Delta t$  = timestep, [t], seconds
- $e$  = regulation error, [m/Lt<sup>2</sup>], Pa
- $f_{pc}(\cdot)$  = production valve characteristic function
- $f_r(\cdot)$  = flow of oil from reservoir into tubing as function of pressure difference, [m/t], kg/s
- $g$  = acceleration of gravity, [L/t<sup>2</sup>], m/s<sup>2</sup>
- $K_P$  = controller gain
- $L_a$  = length of annulus, [L], m
- $L_r$  = length of tubing below gas-injection point, [L], m
- $L_w$  = length of tubing above gas-injection point, [L], m
- $M$  = molar weight of gas, [m/n], kg/mol
- $p_a$  = pressure at the gas-injection point in the annulus, [m/Lt<sup>2</sup>], Pa
- $p_r$  = pressure in reservoir, [m/Lt<sup>2</sup>], Pa
- $p_s$  = pressure in the manifold, [m/Lt<sup>2</sup>], Pa

- $p_{wh}$  = pressure at wellhead, [m/Lt<sup>2</sup>], Pa
- $p_{wb}$  = pressure at wellbore, [m/Lt<sup>2</sup>], Pa
- $p_{wi}$  = pressure at gas-injection point in tubing, [m/Lt<sup>2</sup>], Pa
- $R$  = universal gas constant, [mL<sup>2</sup>/nTt<sup>2</sup>], J/Kmol
- $r_{go}$  = gas/oil ratio in flow from reservoir
- $\rho_{a,i}$  = density of gas at injection point in annulus, [m/L<sup>3</sup>], kg/m<sup>3</sup>
- $\rho_m$  = density of mixture at wellhead, [m/L<sup>3</sup>], kg/m<sup>3</sup>
- $\rho_o$  = density of oil, [m/L<sup>3</sup>], kg/m<sup>3</sup>
- $T$  = time, [t], seconds
- $T_a$  = temperature in annulus, [T], K
- $T_w$  = temperature in tubing, [T], K
- $u$  = setting of production choke
- $v_o$  = specific volume of oil, [L<sup>3</sup>/m], m<sup>3</sup>/kg
- $V_a$  = volume of annulus, [L<sup>3</sup>], m<sup>3</sup>
- $w_{gc}$  = flow of gas into annulus, [m/t], kg/s
- $w_{iv}$  = flow of gas from annulus into tubing, [m/t], kg/s
- $w_{pc}$  = flow of mixture from tubing, [m/t], kg/s
- $w_{po}$  = flow of oil from tubing, [m/t], kg/s
- $w_{pg}$  = flow of gas from tubing, [m/t], kg/s
- $w_{ro}$  = flow of oil from reservoir into tubing, [m/t], kg/s
- $w_{rg}$  = flow of gas from reservoir into tubing, [m/t], kg/s
- $x_1$  = mass of gas in annulus, [m], kg
- $x_2$  = mass of gas in tubing, [m], kg
- $x_3$  = mass of oil in tubing, [m], kg
- $\tau_I$  = controller integral action [t], s

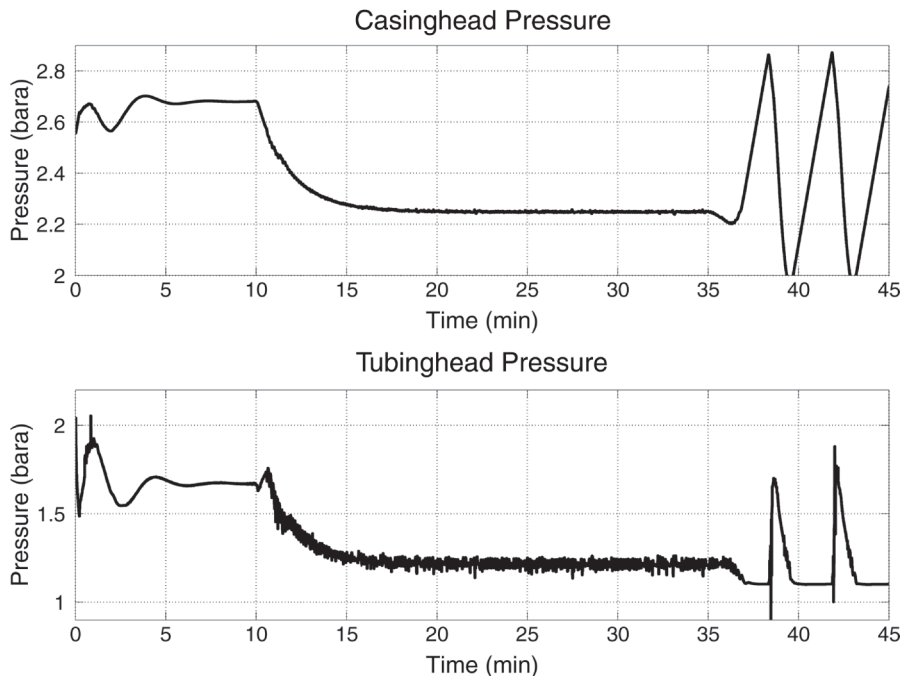


Fig. 12—(a) Casinghead pressure and (b) tubinghead pressure for simulation with OLGA 2000.

**TABLE 5—CONTROL SEQUENCE FOR EXPERIMENTS**

| Time Slot    | Control Mode | Choke Opening |
|--------------|--------------|---------------|
| (-5)–0.5 min | Open loop    | 55.0%         |
| 0.5–25 min   | Closed loop  | Controlled    |
| 25–35 min    | Open loop    | 82.9%         |

**TABLE 6—CONTROLLER PARAMETERS FOR PI-CONTROLLER USED IN THE EXPERIMENTS**

| Choke Opening            | Gain $K_P$ | Integral Time $\tau_I$ |
|--------------------------|------------|------------------------|
| $55\% \leq u \leq 75\%$  | 0.5        | 100 sec                |
| $75\% \leq u \leq 83\%$  | 1.0        | 100 sec                |
| $83\% \leq u \leq 100\%$ | 1.5        | 150 sec                |

**References**

Aamo, O.M., Eikrem, G.O., Siahaan, H., and Foss, B.A. 2005. Observer Design for Multiphase Flow in Vertical Pipes With Gas Lift—Theory and Experiments. *Journal of Process Control* **15** (3) 247–257. DOI: 10.1016/j.jprocont.2004.07.002.

Boisard, O., Makaya, B., Nzossi, A., Hamon, J.C., and Lemetayer, P. 2002. Automated Well Control Increases Performance of Mature Gas lifted Fields, Sendji Case. Paper SPE 78590 presented at the SPE Abu Dhabi International Petroleum Exhibition and Conference, Abu Dhabi, UAE., 13–16 October. DOI: 10.2118/78590-MS.

Dalsmo, M., Halvorsen, E., and Slupphaug, O. 2002. Active Feedback Control of Unstable Wells at the Brage Field. Paper SPE 77650 presented at the SPE Annual Technical Conference and Exhibition, San Antonio, Texas, 29 September–2 October. DOI: 10.2118/77650-MS.

der Kinderen, W.J.G.J. and Dunham, C.L. 1998. Real-Time Artificial Lift Optimization. Paper SPE 49463 presented at the SPE Abu Dhabi International Petroleum Exhibition and Conference, Abu Dhabi, UAE., 11–14 November. DOI: 10.2118/49463-MS.

Eikrem, G.O., Aamo, O.M., and Foss, B.A. 2006. Stabilization of Gas-Distribution Instability in Single Point Dual Gas lift Wells. *SPEPO* **21** (2): 252–259. SPE-97731-PA. DOI: 10.2118/97731-PA.

Fairuzov, Y.V. et al. 2004. Stability Maps for Continuous Gas lift Wells: A New Approach to Solving an Old Problem. Paper SPE 90644 presented at the SPE Annual Technical Conference and Exhibition, Houston, 26–29 September. DOI: 10.2118/90644-MS.

Franklin, G.F., Powell, J.D., and Emami-Naeini, A. 2002. *Feedback Control of Dynamic Systems*. Upper Saddle River, New Jersey: Prentice-Hall.

Hu, B. and Golan, M. 2003. Gas lift Instability Resulted Production Loss and Its Remedy by Feedback Control: Dynamical Simulation Results. Paper SPE 84917 presented at the SPE International Improved Oil Recovery Conference in Asia Pacific, Kuala Lumpur, 20–21 October. DOI: 10.2118/84917-MS.

Jansen, B. et al. 1999. Automatic Control of Unstable Gas Lifted Wells. Paper SPE 56832 presented at the SPE Annual Technical Conference and Exhibition, Houston, 3–6 October. DOI: 10.2118/56832-MS.

Poblano, E., Camacho, R., and Fairuzov, Y.V. 2005. Stability Analysis of Continuous-Flow Gas Lift Wells. *SPEPF* **20** (1): 70–79. SPE-77732-PA. DOI: 10.2118/77732-PA.

Xu, Z.G. and Golan, M. 1989. Criteria For Operation Stability of Gas lift Wells. Paper SPE 19362 available from SPE, Richardson, Texas.

**SI Metric Conversion Factors**

|                              |                       |
|------------------------------|-----------------------|
| bar × 1.0*                   | E+05 = Pa             |
| bara (bara+1) × 1.0*         | E+05 = Pa             |
| bbbl × 1.589 873             | E–01 = m <sup>3</sup> |
| Btu × 1.055 056              | E+00 = kJ             |
| ft × 3.048*                  | E–01 = m              |
| ft <sup>2</sup> × 9.290 304* | E–02 = m <sup>2</sup> |
| ft <sup>3</sup> × 2.831 685  | E–02 = m <sup>3</sup> |
| °F (°F+459.67)/1.8           | = K                   |
| lbm × 4.535 924              | E–01 = kg             |

\*Conversion factor is exact.

**Appendix—Detailed Modeling**

The flows occurring in the model of Eqs. 1 through 3 are modeled by

$$w_{gc} = \text{constant flow rate of lift gas, } \dots\dots\dots (A-1)$$

$$w_{iv} = C_{iv} \sqrt{\rho_{a,i} \max\{0, p_{a,i} - p_{wi}\}}, \dots\dots\dots (A-2)$$

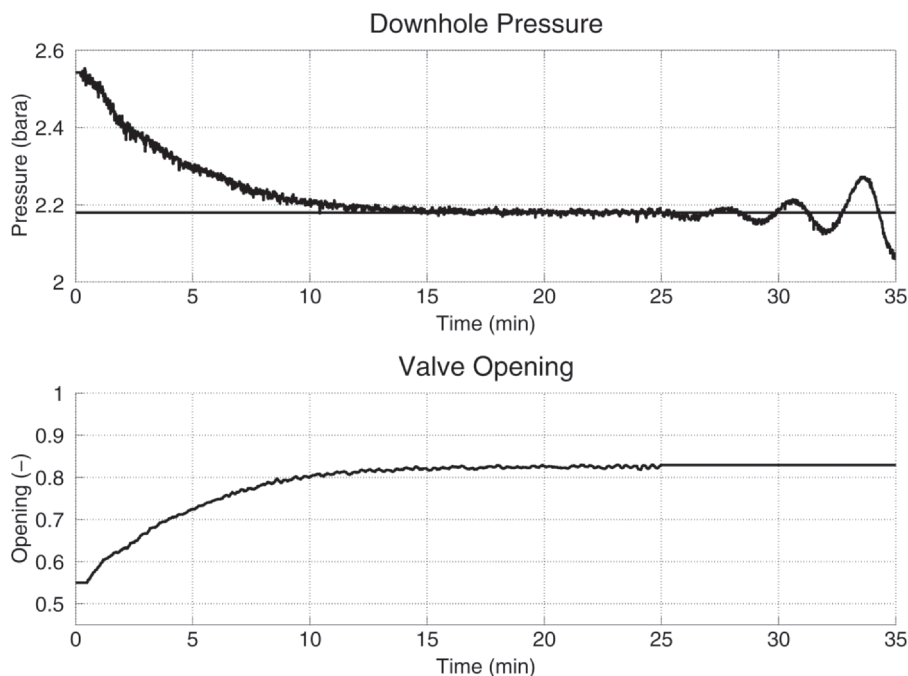


**Fig. 13—(a) Downhole pressure and (b) production-choke opening for laboratory experiment.**

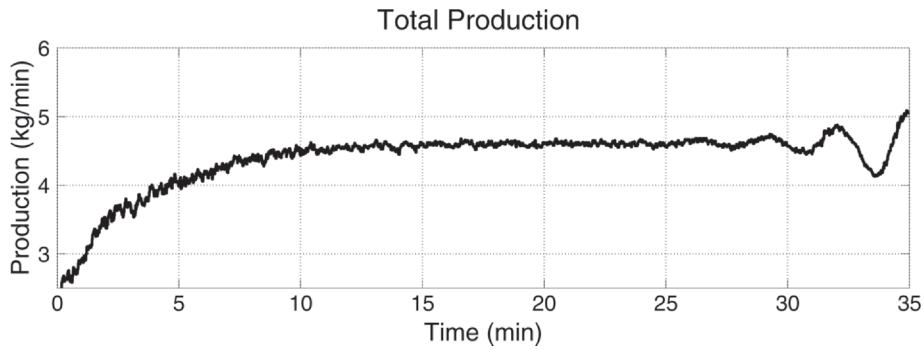


Fig. 14—Total production for laboratory experiment.

$$w_{pc} = C_{pc} \sqrt{\rho_m \max\{0, p_{wh} - p_s\} f_{pc}(u)}, \dots \dots \dots (A-3)$$

$$w_{pg} = \frac{x_2}{x_2 + x_3} w_{pc}, \dots \dots \dots (A-4)$$

$$w_{po} = \frac{x_3}{x_2 + x_3} w_{pc}, \dots \dots \dots (A-5)$$

$$w_{ro} = f_r(p_r - p_{wb}), \dots \dots \dots (A-6)$$

$$w_{rg} = r_{go} w_{ro}, \dots \dots \dots (A-7)$$

$C_{iv}$  and  $C_{pc}$  are constants,  $u$  is the production choke setting ( $u(t) \in [0, 1]$ ),  $\rho_{a,i}$  is the density of gas in the annulus at the injection point,  $p_{a,i}$  is the pressure in the annulus at the injection point,  $\rho_m$  is the density of the oil/gas mixture at the wellhead,  $p_{wh}$  is the pressure at the wellhead,  $p_{wi}$  is the pressure in the tubing at the gas-injection point,  $p_{wb}$  is the pressure at the wellbore,  $p_s$  is the pressure in the manifold,  $p_r$  is the reservoir pressure far from the well, and  $r_{go}$  is the gas/oil-ratio (on the basis of mass flows) of the flow from the reservoir. The function  $f_{pc}$  is valve-specific and represents a possibly nonlinear scaling of the flow as a function of the choke setting  $u$ .  $f_r$  is a case-specific, possibly nonlinear, mapping from the pressure difference between the reservoir and the wellbore to the fluid flow from the reservoir. The manifold pres-

sure,  $p_s$ , is assumed to be held constant by a control system, and the reservoir pressure,  $p_r$ , and gas/ratio,  $r_{go}$ , are assumed to be varying slowly and are, therefore, treated as constant. Note that flow rates through the valves are restricted to be positive. The densities are modeled as follows:

$$\rho_{a,i} = \frac{M}{RT_a} p_{a,i}, \dots \dots \dots (A-8)$$

$$\rho_m = \frac{x_2 + x_3}{L_w A_w}, \dots \dots \dots (A-9)$$

and the pressures are modeled as follows:

$$p_{a,i} = \left( \frac{RT_a}{V_a M} + \frac{gL_a}{V_a} \right) x_1, \dots \dots \dots (A-10)$$

$$p_{wh} = \frac{RT_w}{M} \frac{x_2}{L_w A_w - v_o x_3}, \dots \dots \dots (A-11)$$

$$p_{wi} = p_{wh} + \frac{g}{A_w} (x_2 + x_3), \dots \dots \dots (A-12)$$

$$p_{wb} = p_{wi} + \rho_o g L_r, \dots \dots \dots (A-13)$$

$M$  is the molar weight of the gas,  $R$  is the gas constant,  $T_a$  is the temperature in the annulus,  $T_w$  is the temperature in the tubing,  $V_a$

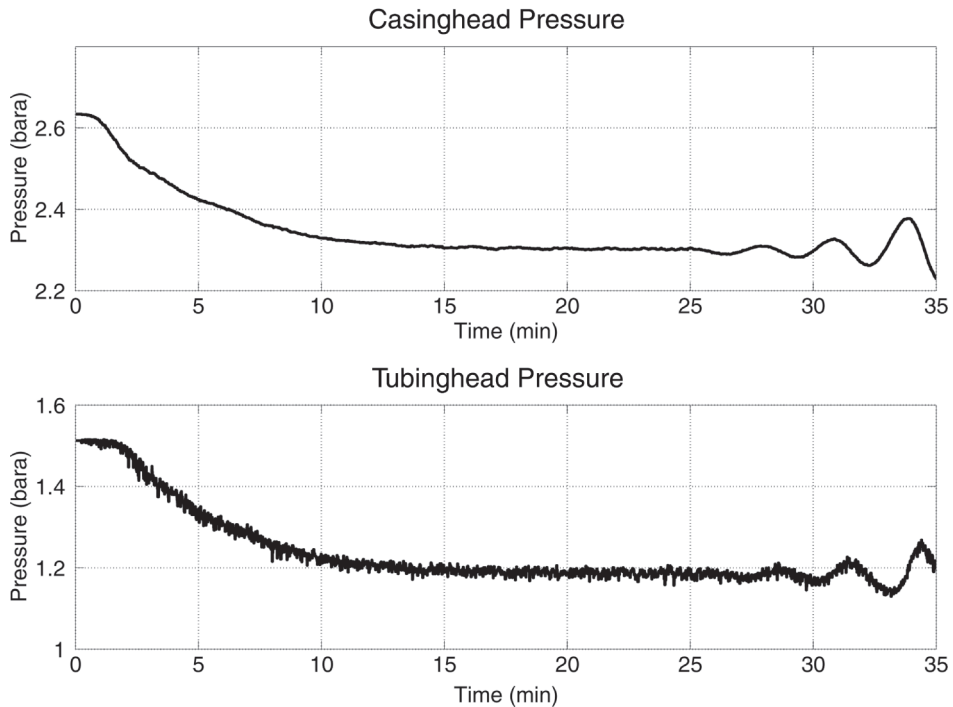


Fig. 15—(a) Casinghead pressure and (b) tubinghead pressure for laboratory experiment.

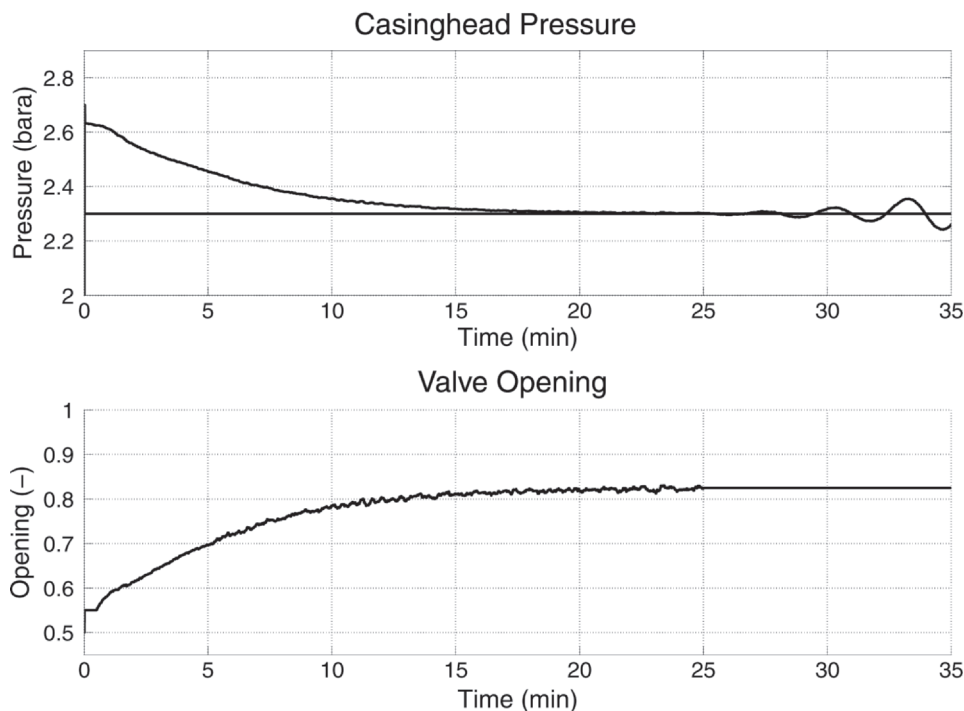


Fig. 16—Experimental results controlling casinghead pressure.

is the volume of the annulus,  $L_a$  is the length of the annulus,  $L_w$  is the length of the tubing above the injection point,  $A_w$  is the cross-sectional area of the tubing above the injection point,  $L_r$  is the length from the reservoir to the gas injection point,  $A_r$  is the cross-sectional area of the tubing below the injection point,  $g$  is the gravity constant,  $\rho_o$  is the density of the oil, and  $\nu_o$  is the specific volume of the oil. The oil is considered incompressible, so  $\rho_o = 1/\nu_o$  is constant. The temperatures,  $T_a$  and  $T_w$ , are slowly varying and are, therefore, treated as constants.

The model presented above is a slight extension of an existing model for gas lift wells (Aamo et al. 2005). This model, as well as

an extended version for single-point dual gas lift wells, (Eikrem et al. 2005) has been validated experimentally.

**Gisle Otto Eikrem** is currently a researcher at the StatoilHydro Research Centre Trondheim in Norway. Eikrem holds a MSc degree in chemical engineering in 2000 and a PhD in engineering cybernetics in 2006, both from the Norwegian University of Science and Technology (NTNU). He has research interests that include process control with special emphasis on flow assurance. **Ole Morten Aamo** is currently a professor with the Norwegian University of Science and Technology (NTNU).

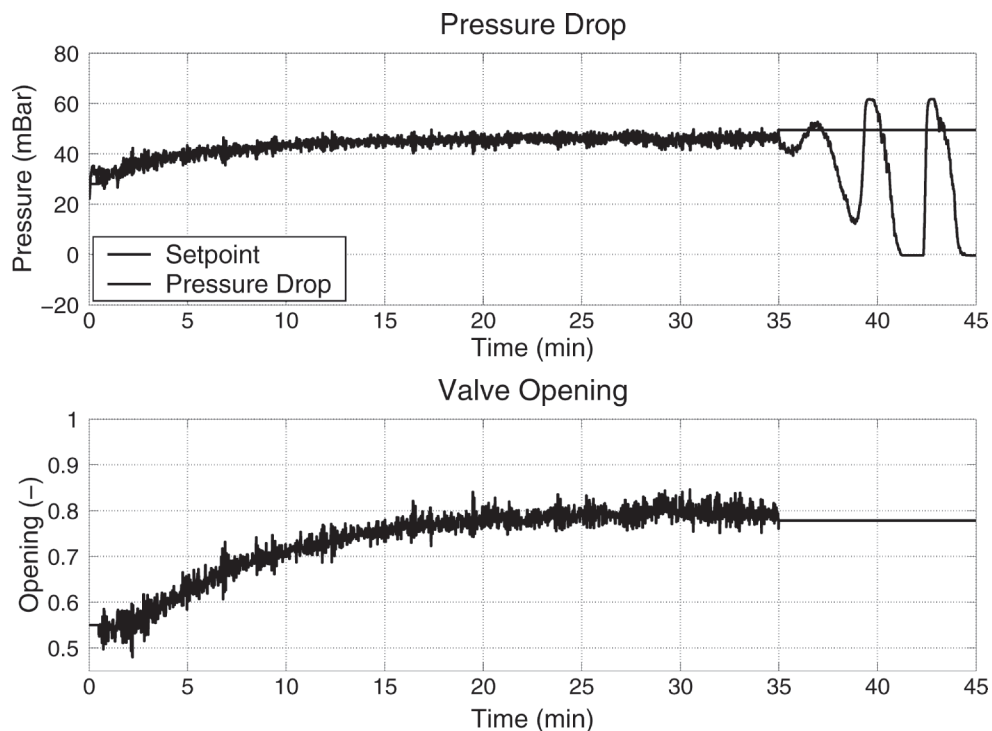


Fig. 17—Experimental results controlling differential pressure.

Aamo holds MSc and PhD degrees in engineering cybernetics from NTNU in 1992 and 2002, respectively. He is a coauthor of the book *Flow Control by Feedback* (Springer-Verlag, 2003) with research interests that include control of distributed parameter systems with special emphasis on fluid flows and applications in the petroleum industry. **Bjarne A. Foss** is a professor at the department of engineering cybernetics at the Norwegian University of Science and Technology (NTNU) since 1989. Foss holds a PhD from the same institution in 1987. He has been

a visiting professor at the University of Texas at Austin. His main interests are in control theory and applications within the process and petroleum-related industries. He is a cofounder of two companies Cybernetica AS and Cyberlab.org AS. Currently he is a program leader at the IO-center at NTNU, SINTEF and IFE. He is a senior member of IEEE, associate editor of *Journal of Process Control*, and member of The Norwegian Academy of Technical Sciences and The Royal Norwegian Society of Sciences and Letters.